Establishment of soil moisture model based on hyperspectral data and growth parameters of winter wheat

Xizhi Lyu[1,2], Weimin Xing[3], Yuguo Han[1,4,5*], Zhigong Peng[4,5], Baozhong Zhang[6,7], Muhammad Roman[1,4,5]

(1. *Key Laboratory of State Forestry Administration on Soil and Water Conservation, College of Soil and Water Conservation, Beijing Forestry University, Beijing 100083, China*;
2. *Yellow River Institute of Hydraulic Research, Key Laboratory of the Loess Plateau Soil Erosion and Water Loss Process and Control of Ministry of Water Resources, Zhengzhou 450003, China*;
3. *College of Hydraulic Science and Engineering, Yangzhou University, Yangzhou 225009, China*;
4. *Forest Ecosystem Studies, National Observation and Research Station, Jixian, Shanxi 042200, China*;
5. *Key Laboratory of Non-point Source Pollution Control, Ministry of Agriculture and Rural Affairs, Beijing 100081, China*;
6. *State Key Laboratory of Simulation and Regulation of Water Cycle in River Basin, China Institute of Water Resources and Hydropower Research, Beijing 100038, China*;
7. *National Center of Efficient Irrigation Engineering and Technology Research-Beijing, Beijing 100048, China*)

Abstract: Large area of soil moisture status diagnosis based on plant canopy spectral data remains one of the hot spots of agricultural irrigation. However, the existing soil water prediction model constructed by the spectral parameters without considering the plant growth process will inevitably increase the prediction errors. This study carried out research on the correlations among spectral parameters of the canopy of winter wheat, crop growth process, and soil water content, and finally constructed the soil water content prediction model with the growth days parameter. The results showed that the plant water content of winter wheat tended to decrease during the whole growth period. The plant water content had the best correlations with the soil water content of the 0-50 cm soil layer. At different growth stages, even if the soil water content was the same, the plant water content and characteristic spectral reflectance were also different. Therefore, the crop growing days parameter was added to the model established by the relationships between characteristic spectral parameters and soil water content to increase the prediction accuracy. It is found that the determination coefficient (R^2) of the models built during the whole growth period was greatly increased, ranging from 0.54 to 0.60. Then, the model built by OSAVI (Optimized Soil Adjusted Vegetation Index) and *Rg*/*Rr*, two of the highest precision characteristic spectral parameters, were selected for model validation. The correlation between OSAVI and soil water content, *Rg*/*Rr*, and soil water content were still significant (p<0.05). The R^2, MAE, and RMSE validation models were 0.53 and 0.58, 3.19 and 2.97, 4.76 and 4.41, respectively, which was accurate enough to be applied in a large-area field. Furthermore, the upper and lower irrigation limit of OSAVI and Rg/Rr were put forward. The research results could guide the agricultural production of winter wheat in northern China.

Keywords: winter wheat, canopy spectra, growth process, soil water content, irrigation threshold, soil moisture model prediction

DOI: 10.25165/j.ijabe.20231603.7268

Citation: Lyu X, Xing W M, Han Y G, Peng Z G, Zhang B Z, Roman M. Establishment of soil moisture model based on hyperspectral data and growth parameters of winter wheat. Int J Agric & Biol Eng, 2023; 16(3): 160–168.

1 Introduction

Soil moisture content is an important factor influencing the crop growth process. It controls the physiological and ecological crop growth process by influencing the changes in crop morphology structure, ultimately affecting agricultural product yield and quality[1,2]. To avoid negative impacts, a timely and accurate assessment of crop water status is necessary to establish appropriate crop water management strategies. Traditionally, crop water status is mainly determined by soil moisture status. Based on the relevant theories of soil physics, many methods, including the drying method, electrical resistance method, neutron scattering method, time-domain reflectometer method, etc., have been developed to measure the soil water content[3-5]. These methods can be easily performed in small-scale areas to get high-precision results. However, it isn't easy to realize the large-scale, comprehensive, and rapid crop water diagnosis using these methods. Therefore, developing a monitoring method of plant or soil moisture content suitable for the large-scale area is of great significance for the guidance of agricultural irrigation, thereby protecting regional food production safety.

Remote sensing technology was first introduced into the agricultural field in the 1980s. Then this technology has been widely used because of its large detection range, various means of

Received date: 2022-07-09 **Accepted date:** 2022-10-27

Biographies: Xizhi Lyu, PhD, Professor, research interest: soil and water conservation, Email: nihulvxizhi@163.com; **Weimin Xing**, PhD, Associate Professor, research interest: soil and water conservation, Email: xingweimin@yzu.edu.cn; **Zhigong Peng**, PhD, Professor, research interest: precision agricultural aviation application, Email: pengzhg@iwhr.com; **Baozhong Zhang**, PhD, Professor, research interest: precision agricultural aviation application, Email: zhangbaozhong333@163.com; **Muhammad Roman**, PhD candidate, research interest: soil and water conservation, Email: m.maan26@outlook.com.

***Corresponding author: Yuguo Han**, PhD, Professor, research interest: agricultural soil and water engineering and nutrient non-point source pollution. School of Soil and Water Conservation, Beijing Forestry University, Beijing 100083, China. Tel./Fax: +86-10-62336635. Email: yghan@bjfu.edu.cn.

obtaining information, and a large amount of relevant information[6,7]. Meanwhile, a weak change of crop water will greatly impact the spectral reflectance of the canopy, making it possible to exploit remote sensing technology for real-time, fast, and accurate diagnosis of crop water content. The spectral features of the leaf and canopy are considered two of the most important indicators to reflect the crop water status[8,9]. However, the spectral values of leaves are relatively difficult to measure and may differ in different positions of the crops, which limits the application of the leaf spectrum in guiding large-scale agricultural irrigation. Whereas the large area of agricultural soil water monitoring has mainly tended to be based on satellite technology and spectrum technology nowadays, it is hard to clarify the connections between leaf spectrum and satellite data. Hence, spectral data of the canopy will be widely promoted from the perspective of application in large areas. Previous studies mainly focused on the sensitive spectral values and ranges of water content. The spectral characteristics of the canopy of wheat, sorghum, and soybean in different growth periods have been studied[10-12]. Ollinger put forward the possible influencing factors of reflectance characteristics of rop canopy[13]. Dobrowski et al. found that the canopy spectrum at 690 nm and 740 nm could reflect the water stress state of plants[14]. Generally, it is believed that the spectral absorption range of water covers near-infrared and short-wave infrared (NIR & SWIR), and the significant absorption peaks (valleys) are 690 mm, 740 mm, 970 mm, 1200 mm, 1450 mm, 1950 mm, and 2250 nm, with slight differences among different plant types[15,16].

After clarifying the sensitive spectrum of water content, the feasibility of using spectral reflectance to diagnose crop water status has been evaluated. At present, there are two major methods to estimate crop water content: 1) establish a multiple regression prediction model with a statistical analysis method based on the correlations between crop water content and spectral reflectance data or its transformation form (such as first derivative, second derivative, logarithmic transformation, etc.), or the combination of spectral data in different wavebands[17,18]; 2) establish relationships between the crop water content and the wavelength variation or other corresponding parameters[19,20]. Most of the existing models' are built water prediction models by selecting spectral parameters, which mostly correlate with the water content of leaves or canopy. However, the plant physiological indicators and water status of plants are changing every day during the crop growth period, indicating that the same spectral value or spectral parameter in different crop growth periods may represent different crop water or soil moisture status, which has been rarely considered in previous studies. Some water content estimation models considering the crop growth periods have also been constructed[21,22]. But the crop growth periods are usually divided based on the agronomic field. Segmented functions have to be founded to best fit the data in each growth period, leading to the varying spectral parameters and fuzzy boundaries of growth periods in these models, which is not conducive to the final application.

In this study, the winter wheat, which is widely planted in north China and sensitive to water conditions, was selected to carry out a field experiment to 1) build a soil water content prediction model based on screening characteristic spectral parameters with crop growth process taking into consideration; 2) propose the lower threshold values of spectral parameters in different growth periods of winter wheat to guide agricultural irrigation under the optimal irrigation system. This work will provide a theoretical supplement for using remote sensing data to predict soil water content and contribute to the guidance of large-scale agricultural irrigation.

2 Materials and methods

2.1 Study area

The field experiment was carried out at the Daxing irrigation experiment station (39°39'N, 116°15'E). This area belongs to a semi-arid temperate continental monsoon climate. It is cold and snowy in winter, and hot and rainy in summer. The average annual precipitation is 540 mm. The precipitation is mainly concentrated from June to September, accounting for up to 80% of the annual precipitation. The soil texture was classified as sandy loam, and the soil properties are listed in Table 1.

Table 1 Soil properties in Daxing irrigation experiment station

Particle contents/%			Soil Type	Soil bulk density/ $g \cdot m^{-3}$	Saturated moisture/ %	Field capacity/ V%
<0.002 mm	0.002-0.02 mm	0.02-2 mm				
1.30	42.70	56.00	Sandy loam	1.41	45.60	33.00

2.2 Experimental design

The variety of winter wheat planted in this experiment was "Jingdong 22". The date and amount of irrigation in different treatments are listed in Table 2. The experiment was set to be a randomized complete block design.

Table 2 Irrigation date and amount of different treatments (mm)

Irrigation date		Treatment and irrigation amount				
		W0	W1	W2	W3	W4
2016-2017	2016/11/8	0	0	60	60	60
	16 d (2017/3/27)	0	0	0	0	60
	29 d (2017/4/9)	0	60	60	60	60
	53 d (2017/5/3)	0	0	0	60	60
	Total	0	60	120	180	240
2017-2018	2017/11/9	0	0	60	60	60
	20 d (2018/3/30)	0	0	0	0	60
	46 d (2018/4/25)	0	60	60	60	60
	62 d (2018/5/11)	0	0	0	60	60
	Total	0	60	120	180	240
2018-2019	2018/11/13	0	0	60	60	60
	17 d (2019/3/28)	0	0	0	0	60
	43 d (2019/4/23)	0	60	60	60	60
	60 d (2019/5/10)	0	0	0	60	60
	Total	0	60	120	180	240

Note: In 2016-2017, the dates of sowing, sprouting, overwinter water irrigating, and regreening stage were October 6, 2016, October 8, 2016, November 8, 2016, and March 12, 2017 (first day of growth), respectively. In 2017-2018, the dates were October 13, 2017, October 22, 2017, November 9, 2017, and March 10, 2018 (first day of growth), respectively, and were October 11, 2018, October 21, 2018, November 13, 2018, and March 12, 2019 (first day of growth), respectively in the experiment of 2018-2019.

The irrigation amount was 0, 60, 120, 180, and 240 mm in W0, W1, W2, W3, and W4 treatment, respectively. The irrigation amount each time was 60 mm. Border irrigation was performed by directing water to the experimental plots through pipes. The water was diverted uniformly through the holes in the pipes (hole spacing: 20 cm, and hole diameter: 1.5 cm).

Each treatment had three replicates, with a total of 15 experimental plots. The area of the experimental plot was 7 m×8 m. All of the treatments were arranged randomly. In this study, the first day of regreening in spring was taken as the first day of growth. The corresponding days of the regreening period, jointing period,

heading period, flowering period, and filling period were 1-30 d, 31-45 d, 46-60 d, 61-70 d, and 71-80 d, respectively.

2.3 Measuring methods and indices

The measuring date and frequency of canopy spectrum, plant water content, and soil water content were the same. In the experiment, data collection was carried out every 7-10 d, and the weather determined the final sampling time. The measuring time was from 10:00-14:00 under sunny and windless weather.

2.3.1 Measurement of canopy spectrum

The canopy spectrum of the winter wheat was measured using the Field-Spec HandHeld2 hand-held ground spectrometer manufactured by American Analytical Spectral Device (ASD) with a field of view of 25°, a spectral range of 350-1075 nm, a sampling interval of 1 nm and a spectral resolution of 3 nm. The sensor probe was set vertically downward to the ground, and the vertical height from the target was about 30 cm. Three sampling points were measured in each plot, and the average value was calculated as the spectral reflectance of the experimental plot.

2.3.2 Measurement of the plant water content

After the completion of the canopy spectrum measurement, 5 winter wheat plants were randomly selected from the spectrum-measuring range and collected to determine plant water content. The plant water content was measured by the drying method. Firstly, fresh plant quality was weighed by analytical balance (0.01 g accuracy). Samples were bagged and dried at 105°C for 1 h, and then the dry matter weight of the plant was recorded after it was dried at 75°C to a constant weight. The plant water content could be calculated by

$$w = \frac{(m_1 - m_2)}{(m_1)} \quad (1)$$

where, w is the water content of the sample, %; m_1 is the fresh plant quality of the sample, g; m_2 is the dry matter quality of the sample, g.

2.3.3 Measurement of the soil water content

Soil water content was measured by Time Domain Reflectory (TDR) method. Each plot had three measuring points, and the average value was treated as the soil water content of the experimental plot. The soil water contents were measured at ten soil depths, which were 0-10, 10-20, 20-30, 30-40, 40-50, 50-60, 60-70, 70-100, 100-120, 120-140 cm at each site.

2.4 Statistic analysis methods

The spectral data were converted to spectral reflectance by View-Spe-Pro software. Differential significance analysis was performed using SPSS Statistic 21 software with a 95% confidence interval (ANOVA). The figures were drawn using Excel 2010 software.

The determination coefficient (R^2), root mean square error (RMSE) and mean absolute error (MAE) were used to evaluate the simulation effect between the simulated value and measured value. RMSE and MAE can test the unbiasedness of the models. Lower index values indicate stronger unbiasedness and better simulation results of the model. These indices could be calculated by

$$R^2 = \frac{\sum (y_i - y_i')^2}{\sum (\bar{y}_i - y_i)^2} \quad (2)$$

$$\mathrm{RMSE} = \sqrt{\frac{\sum_{i=1}^{n} (y_i - y_i')^2}{n}} \quad (3)$$

$$\mathrm{MAE} = \frac{\sum_{i=1}^{n} |y_i - y_i'|}{n} \quad (4)$$

where, y_i represents the measured value; y_i' represents the simulated value; N represents the number of samples.

2.5 Model construction based on growth parameters

Characteristic spectral parameter values were calculated based on the measured spectral reflectance data. A soil moisture prediction model was constructed using the characteristic spectral parameter, soil moisture content, and plant growth time by a multiple linear regression method, and the model was screened based on their correlation.

This research selected 22 spectral parameters commonly used in previous studies as the basic parameters to establish the soil moisture prediction models. The specific parameters are listed in Table 3. The characteristic spectral parameters were first selected to build the prediction model of soil water content in different growth periods based on the data in 2017. Afterward, the soil water content prediction models without plant growth period and with plant growth period parameters in the whole growth period were also established respectively. The parameters were then screened, and the prediction effects were evaluated. Additionally, the relatively larger spectral data collection errors of the small canopy during the early stages would result in poor applicability of the models. Therefore, the whole growth period mentioned in the model established in this study did not include the regreening stage period.

Table 3 Review of spectral indices and computational formulas for estimation of water content[8,14,15,19,20]

Spectral index	Computational formula
WI	R970/R900
NWI-1	(R970–R900)/(R970+R900)
NWI-2	(R970–R850)/(R970+R850)
NWI-3	(R970–R880)/(R970+R880)
NWI-4	(R970–R920)/(R970+R920)
NDVI	(R800–R680)/(R800+R680)
OSAVI	1.16 (R800–R670)/(R800+R670+0.16)
D_r	The maximum value of the first derivative spectrum in the red range is 680-760 nm
D_b	The maximum value of the first derivative spectrum in the blue range is 490-530 nm
D_y	The maximum value of the first derivative spectrum in the Yellow range of 560-640 nm
R_g	Maximum band reflectivity in the green range of 510-560 nm
R_r	Minimum band reflectivity in the red range 640-680 nm
SD_r	The area surrounded by the first derivative spectrum in the red range
SD_b	The area surrounded by the first derivative spectrum in the blue edge range
SD_y	The area surrounded by the first derivative spectrum in the range of yellow edge
$(R_g-R_r)/(R_g+R_r)$	Normalized values of green peak reflectivity and Red Valley reflectivity
R_g/R_r	Ratio of Rg to Rr
SD_r/SD_b	Ratio of SDr to SDb
SDr/SD_y	Ratio of SDr to SDy
(SD_r-SD_b)	D-value of SDr to SDb
$(SD_r-SD_b)/(SD_r+SD_b)$	Normalized value of red edge area and blue edge area
$(SD_r-SD_y)/(SD_r+SD_y)$	Normalized value of red edge area and yellow edge area

Note: R means spectral reflectivity of the corresponding band.

3 Results

3.1 Plant water content

The plant water content of winter wheat changing over the whole growth period under different treatments was shown in Figure 1. The plant water content fluctuated with the growth of wheat. According to the data from 2017, 2018, and 2019, the plant water content of all the experimental treatments tended to decrease during the whole growth period. With the data of 2017 as an example, the increase of plant water content on the 37th day might be caused by the fact that winter wheat was in the jointing period when the physiological activities of the plant were vigorous, and the free water and bound water in the plant were both at a high level[23]. The fluctuation of plant water content on the 75th day was mainly due to the increase of grain water content at the filling stage when the grains were formed.

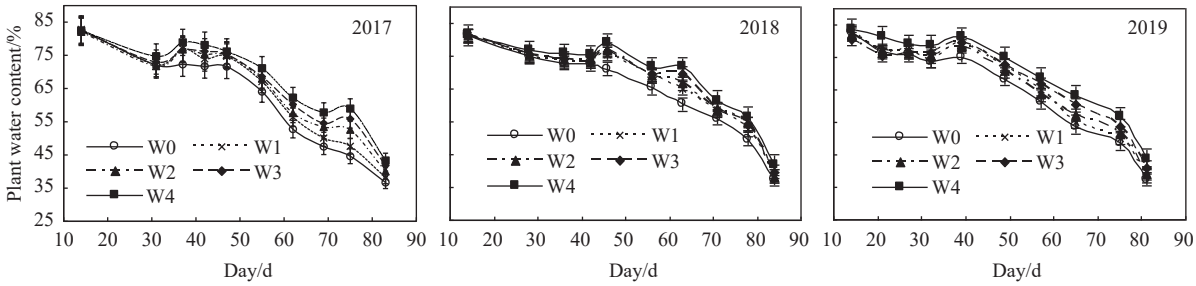

Figure 1 Change of plant water content of winter wheat in 2017, 2018, and 2019

During the whole growth period, the water contents of 2017, 2018, and 2019 were 36.70%-82.79%, 36.05%-81.10%, and 36.10%-81.38%, respectively. In Figure 1, except for 40 d after regreening and the last sampling times, the difference in plant water content among different treatments at other sampling times reached a significant level (p<0.05). The reason why the difference is not significant at the early stage of growth is that the water treatment in the early stage of wheat growth has not been fully carried out, and the reason why the no significant difference in the later stage of the experiment is that the aging of plant cells and tissues would result in poor water retention capacity.

3.2 Correlation between soil water content and plant water content

Plants absorb solar radiation through leaves, and the temperature of leaves gradually rises. At the same time, plants consume water through transpiration to lower the temperature, thereby achieving energy balance. The reduction in the water supply to crops will cause a series of physiological changes such as a decrease in stomatal conductance, a slowdown in transpiration, a decrease in photosynthetic rate, a decrease in heat consumption by transpiration, an increase in sensible heat flux, and an increase in leaf temperature, indicating that the state of energy balance is closely related to the horizontal physiological state and water state of crop leaves[24,25]. Therefore, plant water content is closely related to soil water content, which makes it possible to evaluate plant water content based on soil water content.

However, the plant water content might be mostly correlated with the soil water content of different soil layers in different growth periods due to the dynamic change of plant growth. Therefore, the correlation analysis of plant water content and soil water content in different soil depths and growth periods was carried out to select the optimal soil layer, i.e., the characteristic soil layer, to best represent the plant water status (Figure 2).

There was no obvious characteristic soil layer in the early growth stage of winter wheat (Figure 2a). The distinct soil layers firstly appeared on the 37th day at the depth of 0-10 cm and 10-20 cm.

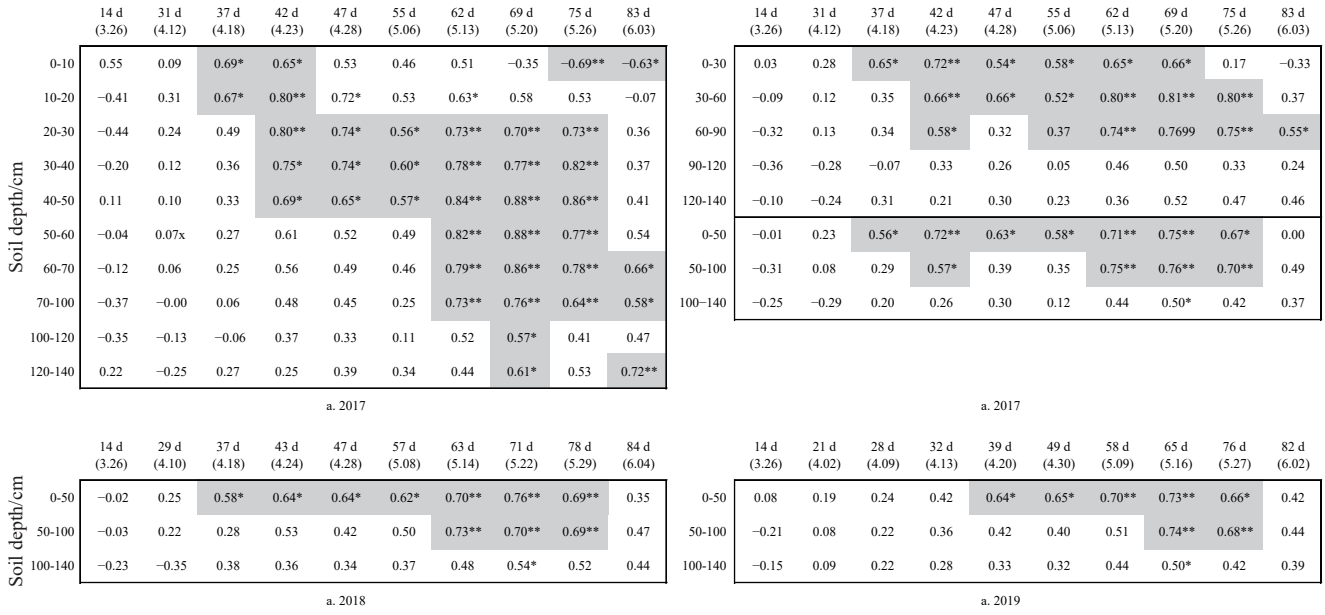

Note: * means significant correlation at 0.05 level and ** means significant correlation at 0.01 level.

Figure 2 Correlation coefficient between soil moisture content and plant water content in different soil depths and in different intervals of soil depths

Then, the depth of distinct soil layers tended to increase with the increase of growth time. Since surface soil water status is greatly affected by external temperature, it cannot fully reflect the overall soil moisture status of plants. Therefore, the correlation between the surface soil water content and plant water content is relatively lower. Another possible reason for this phenomenon was closely related to the growth of plant roots. The depth of plant roots determines which layer of soil water will be absorbed. In the early stage, the plant roots were mainly concentrated on the shallow soil layer, so the depth of the characteristic soil layer was relatively shallow. In the later stage, the roots of winter wheat would enter into the deeper soil layer, increasing the depth of the characteristic soil layer.

The correlation analysis between different interval depths of the soil layer and the plant water content was also conducted to further determine the characteristic soil layer (Figure 2a). It could be shown that the distinct soil layers could reflect the plant water change with small intervals (10 cm, for example), but there were too many relevant characteristic soil layers. While the characteristic soil layer with a large interval (50 cm) was mainly concentrated on a specific soil layer (Figures 2b-2d), the correlations were not detailed enough. For precision irrigation, correlations based on small interval soil layers are suitable for refined farming and management. However, correlations based on a large interval of soil layer are more conducive to guiding large-scale agricultural irrigation for field crops. This work aimed to advise the large-scale agricultural production of winter wheat. Therefore, the characteristic soil layer in this study was selected to be 0-50 cm.

The date of sampling is indicated between parentheses. The soil moisture content corresponding to the soil depth is the average value of the actually measured values or the average value of the measured values of multiple soil layers.

3.3 Correlation among spectral reflectance, soil water content, and plant water content

Previous studies have found that spectral reflectance is closely related to plant water content, while plant water content had significant relationships with soil water content (Figure 2). Therefore, it is feasible to predict plant water content through spectral reflectance, thereby achieving the purpose of estimating soil water content. However, due to the change of plant water content in the whole growth period, even if the soil water content is the same, the spectral reflectance of crops obtained in different growth stages may be different, thus increasing the prediction errors of soil water content. This study selected three data groups with the same soil water content for analysis (Table 4).

Table 4 Spectral characteristics of three groups of samples on different dates under the same soil water content

Year	Date	Treatment	Soil water content/($cm^3 \cdot cm^{-3}$)	Plant water content/%
2017	55 d (2017/5/6)	W1	14.02	63.51
	75 d (2017/5/26)	W2	14.02	48.76
2018	57 d (2018/5/5)	W3	27.67	78.20
	75 d (2018/5/23)	W4	27.67	69.00
2019	32 d (2019/4/12)	W3	23.06	78.12
	55 d (2019/5/5)	W2	23.06	75.48

The soil water content of W1 on the 55th day and W2 on the 75th day in 2017, W3 on the 57th day and W4 on the 75th day in 2018, W3 on the 32nd day and W2 on the 55th day in 2019 were the same, but the plant water contents on the corresponding days were 63.51% and 48.75%, 78.20% and 69.00%, 78.12% and 75.48%, respectively, which testified that the same soil water content might result in different plant water contents in different crop growth stages. Besides, the spectral data of these two treatments at the same period also showed that although the soil water contents had the same values, the corresponding spectral reflectance curves were still different (Figure 3). Therefore, the prediction of soil water content based on spectral reflectance must be combined with plant growth days. Otherwise, large prediction errors may be unavoidable.

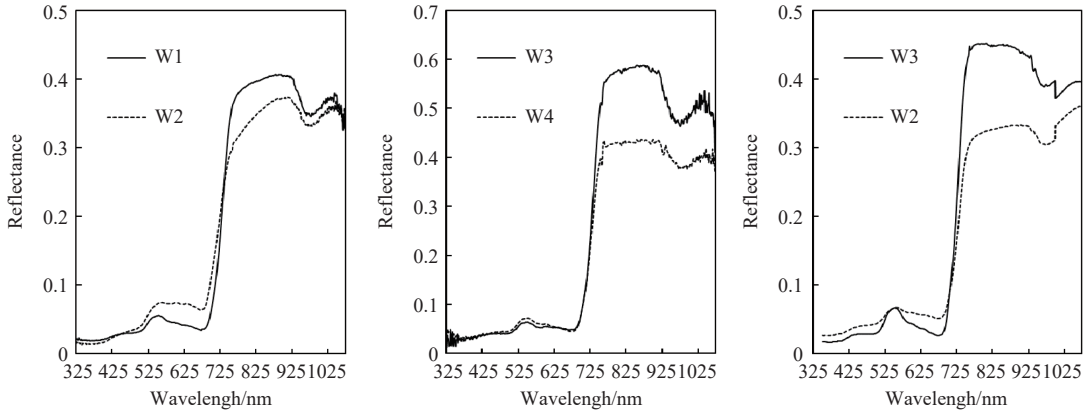

Figure 3 Spectral characteristics of three groups of samples on different dates under the same soil water content

3.4 Screen of characteristic spectral parameters and preliminary construction and validation of models

It could be seen from Table 5 that the determination coefficient (R^2) of the prediction models established on the joining stage, heading stage, filling stage, and whole growth period without growing days parameters were 0.01-0.34, 0.00-0.60, 0.01-0.41, 0.00-0.31, respectively. After adding the growing days' parameter, the R^2 was significantly increased, ranging from 0.54 to 0.60. Therefore, adding the growing days' parameter could be beneficial to improve the accuracy of predicting soil water content based on canopy spectral parameters.

In order to test the reliability of the model, the model was constructed by two high-precision parameters, namely OSAVI (OSAVI Computational formula $1.16\times(R_{800}-R_{670})/(R_{800}+R_{670}+0.16)$, R means spectral reflectivity of the corresponding band) and R_g/R_r (R_g means maximum band reflectivity in the green range of 510-560 nm, R_r means minimum band reflectivity in the red range 640-680 nm), with growing days parameter and without growing days parameter during the whole growth period was respectively verified based on the data of 2018 and 2019 (Figure 4). The R^2 of models

Table 5 Fitting equations and R^2 of models established based on different spectral indices during the jointing stage, heading stage, filling stage, and the whole growth stages (with/without growth days' parameters)

Index	Jointing stage		Heading stage		Filling stage		Whole stage (without the growth days parameter)		Whole stage (with growth days parameter)	
	Equation	R^2	Equation	R^2	Equation	R^2	Equation	R^2	Equation	R^2
WI	y=109.59x–70.93	0.14	y=–192.46x+178.27	0.59	y=–30.74x+41.53	0.37	y=61.85x–32.17	0.05	y=–11.41x–0.25d+41.77	0.55
NWI–1	y=190.40x+37.65	0.14	y=–325.85x–11.76	0.59	y=–54.18x+11.01	0.38	y=103.82x+28.83	0.04	y=–21.08x–0.25d+30.36	0.55
NWI–2	y=180.38x+36.75	0.10	**y=–273.80x–5.99**	**0.60**	y=–41.09x+12.31	0.39	**y=27.65x+22.61**	**0.00**	y=–21.99x–0.24d+30.08	0.55
NWI–3	y=190.89x+38.18	0.11	y=–298.52x–9.73	0.59	y=–48.71x+11.38	0.39	y=78.09x+26.93	0.02	y=–24.83x–0.25d+29.90	0.55
NWI–4	y=198.42x+37.54	0.12	y=–380.78x–15.50	0.58	**y=–66.78x+10.26**	**0.41**	y=145.24x+31.70	0.07	y=–20.82x–0.25d+30.50	0.55
NDVI	**y=242.18x–200.33**	**0.34**	y=134.39x–100.41	0.51	y=7.82x+9.07	0.29	y=143.77x–109.13	0.34	y=2.81x–0.24d+28.99	0.55
OSAVI	y=36.21x–5.62	0.04	y=26.16x–1.88	0.05	y=9.05x+9.20	0.27	y=52.68x–19.12	0.26	**y=9.00x–0.21d+23.45**	**0.56**
D_r	y=521.28x+18.05	0.02	y=26.16x–1.88	0.05	y=238.43x+13.35	0.08	y=2 205.90x–0.37	0.29	y=288.87x–0.22d+28.04	0.55
D_b	y=–10.51x+27.72	0.01	y=85.31x–13.72	0.33	y=238.43x+13.35	0.08	y=48.50x+1.59	0.18	y=1 690.66x–0.25d+30.20	0.55
D_y	y=-3 261.60x+27.34	0.04	y=-32 768.00x+48.00	0.00	y=-1 340.00x+16.37	0.03	y=4 477.90x+15.43	0.03	y=-1 247.69x–0.24d+30.57	0.55
R_g	y=–201.26x+27.25	0.03	**y=28.19x+16.08**	**0.00**	y=–173.50x+18.96	0.21	y=233.31x+16.16	0.02	y=–11.36x–0.24d+32.34	0.55
R_r	y=–0.28x+28.04	0.32	y=–0.07x+17.72	0.02	**y=–0.02x+15.09**	**0.01**	y=-6 732.40x+13.82	0.02	y=–13.53x–0.24d+31.84	0.55
SD_r	y=–129.34x+26.12	0.02	y=715.01x+5.24	0.17	y=128.72x+13.51	0.19	y=499.50x+10.96	0.16	y=9.69x–0.22d+26.93	0.55
SD_b	y=–197.09x+32.24	0.16	y=–369.53x+34.72	0.16	y=–59.74x+18.97	0.32	y=–345.33x+36.62	0.20	y=131.42x–0.27d+30.51	0.55
SD_y	y=–711.83x+35.80	0.42	y=–665.49x+34.93	0.46	y=–37.47x+16.87	0.29	y=–704.17x+35.76	0.02	y=85.48x–0.23d+29.47	0.55
(R_g-R_r)/(R_g+R_r)	y=71.12x–8.13	0.48	y=63.82x–1.54	0.48	y=8.87x+13.54	0.35	y=49.60x+1.82	0.39	**y=16.23x–0.12d+20.06**	**0.54**
R_g/R_r	y=10.38x–3.72	0.46	y=16.31x–12.85	0.49	y=3.51x+10.03	0.40	**y=9.49x–1.02**	**0.31**	**y=3.54x–0.10d+18.37**	**0.60**
SD_r/SD_b	y=0.51x+12.36	0.05	y=1.10x–6.62	0.26	y=3.51x+10.03	0.40	y=1.17x–4.58	0.17	y=–0.02x–0.26d+32.64	0.54
SD_r/SD_y	y=0.28x+17.91	0.02	y=–0.22x+21.66	0.02	y=–0.01x+15.08	0.03	y=–0.65x+34.04	0.11	y=0.01x–0.26d+32.24	0.55
(SD_r-SD_b)	**y=–10.70x+27.59**	**0.01**	y=89.19x–13.58	0.34	y=13.77x+11.28	0.22	y=52.59x+0.96	0.19	y=8.57x–0.22d+27.64	0.55
(SD_r-SD_b)/(SD_r+SD_b)	y=102.30x–69.89	0.04	y=–0.22x+21.66	0.02	y=15.01x+2.25	0.22	y=266.13x–221.72	0.15	y=–9.05x–0.27d+41.20	0.55
(SDr-SD_y)/(SD_r+SD_y)	y=50.86x–22.56	0.01	y=–73.20x+83.53	0.03	y=–13.59x+27.49	0.07	y=–157.67x+163.57	0.10	y=–3.76x–0.25d+35.45	0.54

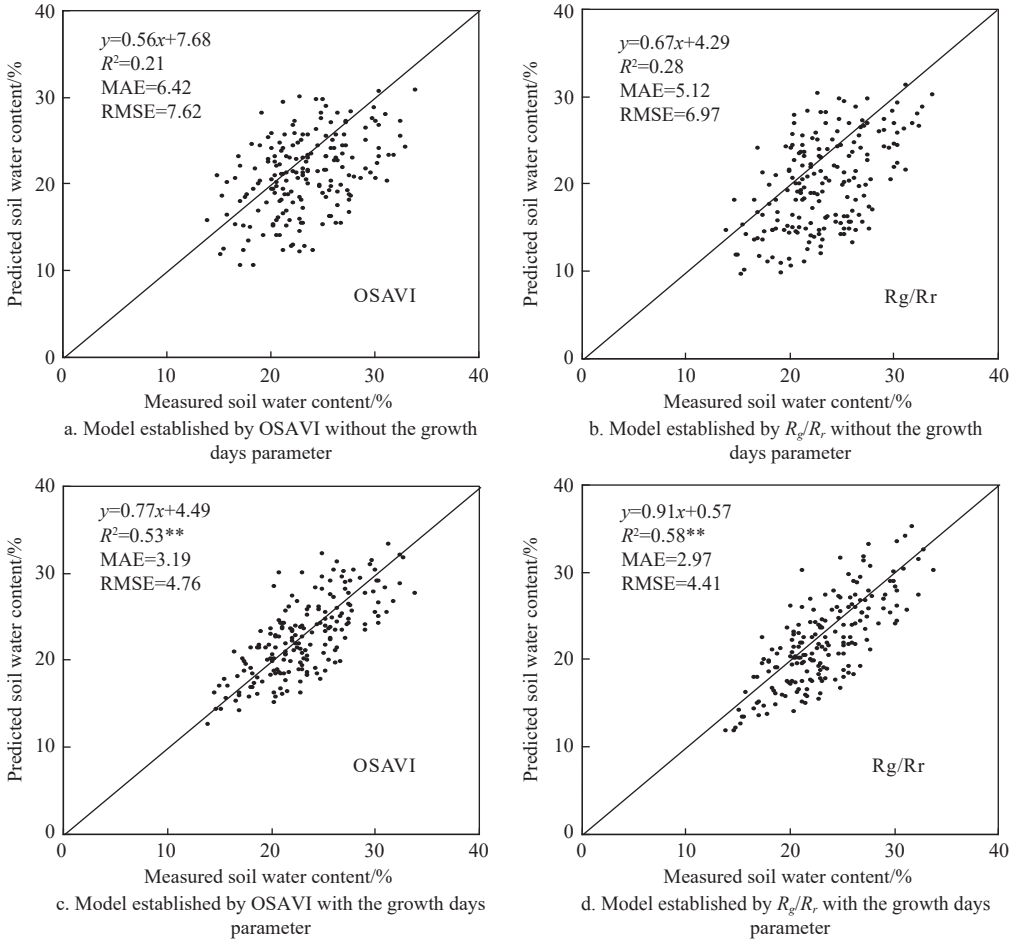

a. Model established by OSAVI without the growth days parameter

b. Model established by R_g/R_r without the growth days parameter

c. Model established by OSAVI with the growth days parameter

d. Model established by R_g/R_r with the growth days parameter

Figure 4 Model validation with data of the whole growth stage of 2018 and 2019

established by OSAVI and R_g/R_r in the whole growth period without days parameters were 0.256 and 0.310, respectively, indicating that the errors of using these two models to predict soil water content were too large to be applied in reality. After adding the day's parameter, the R^2, MAE, and RMSE of the models established by OSAVI and R_g/R_r were 0.53 and 0.58, 3.19 and 2.97, 4.76 and 4.41, respectively. The simulation effect was better compared to that without the day's parameter, which demonstrated that the prediction model of soil water content in the whole growth period of winter wheat based on the growing days' parameter had better applicability.

4 Discussion

Winter wheat is one of the most important field crops in the world. The main purpose of using the spectral index of the canopy to predict soil moisture status is to solve the problem of wheat yield reduction caused by water deficit. Therefore, in order to be applied practically to guide agricultural irrigation, the threshold values of characteristic spectral parameters during the corresponding period should be determined.

Many field experiments have been conducted to determine the threshold values of soil water content. Since our experimental site was located in the north of China, the main research results of winter wheat in this area were reviewed and summarized in Table 6. Zhu and Niu considered that the threshold value of soil water content was 60.40%-65.80% of the field moisture capacity based on the water use efficiency, ear forming rate, number of grains per ear, and the relative yield in jointing-heading stage and the stomatal resistance, photosynthetic intensity, filling speed, growth rate and relative yield in heading-maturation stage[23]. The results of Kang et al.[26] showed that the lower irrigation limit of soil water content in different periods of winter wheat was 42%-60% of field moisture capacity by controlling the photosynthetic rate. Zhang et al.[27] concluded that the threshold of the soil water content of the lower irrigation limit was 55%-65% of field moisture capacity by analyzing the indices of stomatal conductance, leaf water potential, and photosynthetic rate. In summary, there will be some differences in the threshold of soil water content based on different evaluation indices. In addition, previous studies have also found that the root of 0-50 cm soil layer accounts for more than 80% of the total root system of winter wheat, so the research results of Zhang et al.[23,26,27] are selected as the lower and upper irrigation limit of winter wheat in this study.

Table 6 Reviews of the lower irrigation limit of the soil water content of winter wheat in northern China

Area	Soil layer/cm	Growing stage	Threshold/%
Gongxian, Henan Province[23]	0-130	Jointing-heading stage	60.4-78.1
		Heading-maturation stage	65.8-79.6
Xi'an[26]	0-100	Reviving stage	60
		Jointing and heading stage	64
		Filling stage	42
Xinxiang, Henan Province[28]	0-100	Heading stage	65
Shijiazhuang[27]	0-50	Overwintering stage	60-80
		Reviving stage	55-80
		Jointing stage	65-80
		Heading stage	60-80
		Filling stage	60-80
Zhengzhou[29]	0-100	Emergence-overwintering stage	62.5-67.6
		Overwintering-reviving stage	63.4-70.9
		Reviving-jointing stage	64.5-72.2
		Jointing-heading stage	62.4-69.1
		Heading-maturation stage	64.2-72.7

The upper and lower irrigation limits of winter wheat were then introduced into the prediction model to determine the characteristic spectral parameters in different growth periods (Figure 5). The upper dotted lines in Figures 5a and 5b are the upper irrigation limit, and the solid lines are the lower irrigation limit recommended by the model.

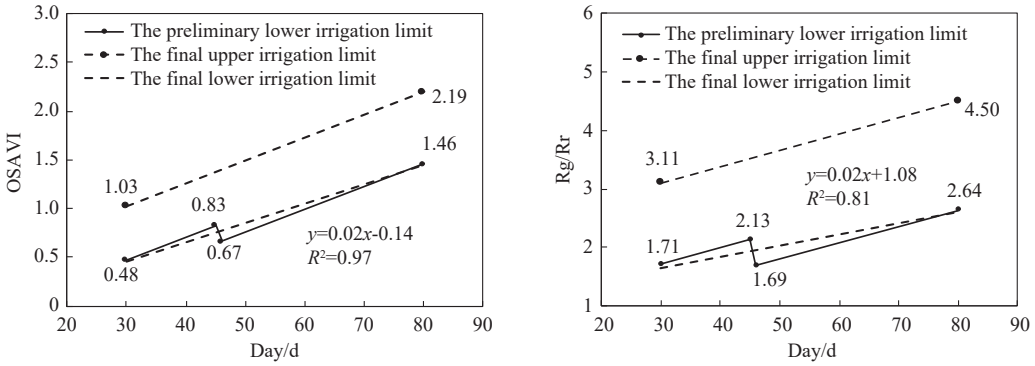

Figure 5 Irrigation upper and lower limits of OSAVI and *Rg*/*Rr* during the growth process of winter wheat, the solid line represents the irrigation lower limit based on the growth period of agronomy, and the dotted line represents the finally recommended irrigation upper and lower limit

There was a jump between the two growth periods due to different lower irrigation limits obtained by previous research when taking the agronomic growth period as the research cycle. However, crop growth is a continuous process in reality. Therefore, the relevant model was fitted twice, and the final model describing the lower irrigation limit of spectral parameters for the whole growth period of winter wheat was shown by the dotted line in the figure. It indicated that water deficit occurred when the corresponding spectral value was lower than this line, and irrigation should be started to ensure the normal growth of the winter wheat until OSAVI or R_g/R_r reached the upper limit value, that is, the irrigation reached the upper limit.

As shown in Figure 5, the interval between the two dotted lines is the optimal soil moisture range for winter wheat. If the value of OSAVI or R_g/R_r is smaller than the lower limit shown in Figure 5, there will be a certain risk of water deficit that may cause a

reduction in production. When the value of OSAVI or R_g/R_r reaches the upper limit after irrigation, the irrigation could be regarded as sufficient enough to be stopped. Once it exceeds the upper irrigation limit, it indicates that the soil moisture is too high, which may cause waterlogging and cause damage to plants, and it should be drained in time. In actual practice, the situation of exceeding the upper limit is rarely caused by irrigation. Generally, it may be caused by rainfall or non-irrigated surface water entering the field. Therefore, the model constructed in this study can provide guidance for irrigation and a basis for field drainage.

5 Conclusions

This research demonstrated that it was feasible to build a model to predict soil moisture status based on spectral parameters of the canopy by clarifying the correlations among a spectral index of the canopy, plant water content, and soil water content. However, due to the change in plant water content, the soil water content represented by the same spectral parameters in different crop growth stages may be different during the whole growth period. Therefore, it is necessary to modify the soil water content prediction model by adding the crop growing days parameter. The results showed that after adding the growing day's parameter, the determination coefficient (R^2) of the prediction model established in the whole growth period increased significantly, ranging from 0.55 to 0.59.

The models built by OSAVI and R_g/R_r, which ranked as two of the highest precise parameters, were selected for model validation. The correlations between OSAVI and soil water content and between R_g/R_r and soil water content were still significant ($p<0.05$). The R^2, MAE, and RMSE of validation models were 0.56 and 0.52, 1.97 and 2.18, 2.82 and 3.37, respectively, which was accurate enough to be applied in large-area fields. Combined with the previous research results, the upper and lower irrigation limit of these two spectral parameters during the whole growth period were constructed, which could be used to guide the agricultural production of winter wheat in Northern China.

Acknowledgements

This study was financially supported by the National Natural Science Foundation of China (Grant No. 31700640), the National Key R&D Program of China (Grant No. 2018YFC0407703), the Key R&D Projects of Ningxia Hui Autonomous Region (Grant No. 2018BBF02022), the IWHR Research & Development Support Program (Grant No. ID0145B082017), Beijing Municipal Education Commission Innovative Transdisciplinary Program "Ecological Restoration Engineering", and the National Key Laboratory Open Fund (Grant No. IWHR-SKL-KF201903).

[References]

[1] Karthikeyan L, Chawla I, Mishra A K. A review of remote sensing applications in agriculture for food security: crop growth and yield, irrigation, and crop losses. Journal of Hydrology, 2020; 586: 124905.

[2] Tan M, Gou F, Stomph T J, Wang J, Werf W V D. Dynamic process-based modelling of crop growth and competitive water extraction in relay strip intercropping: model development and application to wheat-maize intercropping. Field Crops Research, 2020; 246: 107613.

[3] Paul A D, Fanrong J Z, Agnèès D, Jean C M, Randal D K. The sensitivity of surface fluxes to soil water content in three land surface schemes. Journal of Hydrometeorology, 1999; 1: 121–134.

[4] Davidson E A, Belk E, Boone R D. Soil water content and temperature as independent or confounded factors controlling soil respiration in a temperate mixed hardwood forest. Global Change Biology, 2010; 4: 217–227.

[5] Haynes R J, Swift R S. Stability of soil aggregates in relation to organic constituents and soil water content. European Journal of Soil Science, 1990; 41: 73–83.

[6] Jaiswal R K, Saxena R, Mukherjee S. Application of remote sensing technology for land use/land cover change analysis. Journal of the Indian Society of Remote Sensing, 1999; 27: 123–128.

[7] Gong P. Wireless sensor network as a new ground remote sensing technology for environmental monitoring. National Remote Sensing Bulletin, 2007; 11(4): 545–551. (in Chinese)

[8] Clevers J G P W, Kooistra L, Schaepman M E. Estimating canopy water content using hyperspectral remote sensing data. International Journal of Applied Earth Observation and Geoinformation, 2010; 12: 119–125.

[9] Chen J Y, Chen S B, Zhang Z T, Fu Q P, Bian J, Cui T. Investigation on photosynthetic parameters of cotton during budding period by multi-spectral remote sensing of unmanned aerial vehicle. Transactions of the CSAM, 2018; 49(10): 230–239. (in Chinese)

[10] Wang D, Wilson C, Shannon M C. Interpretation of salinity and irrigation effects on soybean canopy reflectance in visible and near-infrared spectrum domain. International Journal of Remote Sensing, 2002; 23: 811–824.

[11] Li H, Zhao C, Yang G, Feng H. Variations in crop variables within wheat canopies and responses of canopy spectral characteristics and derived vegetation indices to different vertical leaf layers and spikes. Remote Sensing of Environment, 2015; 169: 358–374.

[12] Singh S K, Houx III J H, Maw M J, Fritschi F B. Assessment of growth, leaf N concentration and chlorophyll content of sweet sorghum using canopy reflectance. Field Crops Research, 2017; 209: 47–57.

[13] Ollinger S V. Sources of variability in canopy reflectance and the convergent properties of plants. The New phytologist, 2011; 189: 375–394.

[14] Dobrowski S, Pushnik J, Zarco-Tejada P J, Ustin S. Simple reflectance indices track heat and water stress-induced changes in steady-state chlorophyll fluorescence at the canopy scale. Remote Sensing of Environment, 2005; 97: 403–414.

[15] Rollin E M, Milton E J. Processing of high spectral resolution reflectance data for the retrieval of canopy water content information. Remote Sensing of Environment, 1998; 65: 86–92.

[16] Zheng E, Zhang C, Qi Z, Zhang Z. Canopy temperature response to the paddy water content and its relationship with fluorescence parameters and dry biomass. Agricultural Research, 2020; 4: 1–10.

[17] Feng R, Zhang Y S, Yu W Y, Hu W, Wu J W, Ji R P, et al. Analysis of the relationship between the spectral characteristics of maize canopy and leaf area index under drought stress. Acta Ecologica Sinica, 2013; 33: 301–307.

[18] El-Hendawy S, Al-Suhaibani N A, Elsayed S, Hassan W. Potential of the existing and novel spectral reflectance indices for estimating the leaf water status and grain yield of spring wheat exposed to different irrigation rates. Water Resources Management, 2019; 217: 356–373.

[19] El-Hendawy S, Hassan W, Al-Suhaibani N A, Schmidhalter U. Spectral assessment of drought tolerance indices and grain yield in advanced spring wheat lines grown under full and limited water irrigation. Agricultural Water Management, 2017; 182: 1–12.

[20] Gopal K, Rabi N S, Prafull S, Vaishangi B, Himesh P, Sudhir K, et al. Comparison of various modelling approaches for water deficit stress monitoring in rice crop through hyperspectral remote sensing. Agricultural Water Management, 2019; 213: 231–244.

[21] Carpintero E, Mateos L, Andreu A, González-Dugo M P. Effect of the differences in spectral response of mediterranean tree canopies on the estimation of evapotranspiration using vegetation index-based crop coefficients. Agricultural Water Management, 2020; 238: 106201.

[22] Pas I, Calera A, Campos I, Cunha M. Remote sensing for estimating and mapping single and basal crop coefficientes: A review on spectral vegetation indices approaches. Agricultural Water Management, 2020; 233: 106081.

[23] Zhu Z X, Niu X Z. An ecological analysis on soil moisture indices of winter wheat in its main stages. Journal of Applied Meteorological Science, 1987; 2(1): 81–87. (in Chinese)

[24] Mendez-Costabel M, Dokoozlian N. Do plant-based measurements of vine water status accurately reflect soil moisture content? American Journal of Enology and Viticulture, 2009; 60(3): 404.

[25] Zhao C J, Huang W J, Wang Z J, Wang B H, Wang J H. Relationship between canopy water content and temperature of winter wheat under different water and nitrogen treatments. Transactions of the CSAE, 2022; 18(2): 25–28. (in Chinese)

[26] Kang S Z, Cai H J, Zhang F C. Discussion on crop water management for water saving agriculture. Chinese Journal of Hydrology Engineering, 1996; 5(5): 9–17. (in Chinese)

[27] Zhang X Y, Pei D, Hu C S. Index system for irrigation scheduling of winter wheat and Maize in the Piedmont of Mountain Taihang. Transactions of the CSAE, 2002; 18(6): 36–41. (in Chinese)

[28] Wu H Q, Duan A W, Yang C F. Physiological and morphological responses of winter wheat to soil moisture. Acta Agriculturae Boreali-Sinica, 2000; 15(1): 92–96. (in Chinese)

[29] Fang W S, Liu R H, Deng T H. Study on reasonable soil moisture indexes of growth and development for winter wheat. Chinese Journal of Agrometeorology, 2010; 31(S1): 73–76. (in Chinese)